International Journal of Material Forming (2018) 11:855–866
https://doi.org/10.1007/s12289-017-1395-y

ORIGINAL RESEARCH

Effect of internal pressure on springback during low pressure tube hydroforming

Guan-nan Chu[1] · Cai-yuan Lin[1] · Wei Li[1] · Yan-li Lin[1]

Received: 16 August 2017 / Accepted: 27 December 2017 / Published online: 6 January 2018

Abstract
For the existence of bending deformation during low pressure tube hydroforming(LPTH), springback is unavoidable and deteriorate the forming accuracy. In this paper, an analytical model of springback for LPTH was proposed. The simulation and experiment were carried out to investigate the effects of the main factors on the springback, such as internal pressure, corner radius and thickness. The results indicate that, different from expansion deformation, bending forming is the main and basic deformation for tube forced into the required shape during the LPTH. Consequently, springback appears. However, the deformation type has great dependence on the internal pressure, which ensures the internal pressure of the function to reduce the springback. There is a critical pressure which would induce pure bending deformation and result in the largest springback. Consequently, it need try to avoid the critical pressure for the LPTH. On the contrary, whatever the internal pressure is less or bigger than the critical pressure, springback are all decreased. In contrast, it is more effective to decrease the springback when pressure is bigger than the critical pressure. In addition, bigger corner radius can also contribute to decrease the springback because of a much larger tensile force introduced under the same internal pressure. For a definite component, improving internal pressure is the only method to decrease the springback.

Keywords LPTH · Springback · Critical Pressure · Tube

Introduction

Recently, lightweight forming technology has gained increasing attention due to the demand of reduced fuel consumption and improved safety standards [1]. One forming technology used to form lightweight structural component is tube hydroforming where an internal pressure is applied to force the tube to expand into the required shape among a closed die cavity - much like blowing up a balloon [2]. In such forming process, the internal pressure is the only driving force for the plastic deformation, and needs to reach hundreds of MPa. High pressure induced several disadvantages, such as requiring expensive and specialized machinery to handle the extreme pressure, increasing the cost, especially the difficulty in pressure sealing [3], which seriously limit the wide application of this technology.

Therefore, to reduce the internal pressure is always the goal pursued by numerous researchers. Several variations of hydroforming process have been proposed. In 1998, Variform Company put forward a popular technology named as Low Pressure-Sequence Hydroforming (LPSH) [4], which has been widely used in automotive industry. In LPSH process, the tube was first expanded to a preform shape whose circumferences are close to that of the corresponding section of the final component. After then, the preformed tube was pressurized by an internal pressure and crushed into the desired shape among the die cavity as the die closing. Another popular technology was low pressure tube hydroforming (LPTH) [5, 6] put forward by Nikhare. In this method, a fluid filled tube is crushed to the required shape by the action of a punch or a moving die. For there is no expansion deformation, it was mostly used to manufacture the parts with constant perimeters. In LPTH the internal pressure is less than 10% of that required in tube hydroforming. Also, the thickness distributions of the formed products obtained by the crushing processes are much more uniform than those by the hydraulic expansion test [7]. Thus the process is a promising alternative for the forming of high strength steels.

✉ Yan-li Lin
linyanli0616@163.com

[1] School of Materials Science and Engineering, Harbin Institute of Technology at Weihai, Weihai 264209, People's Republic of China

In the aspect of forming mechanism, there is great difference between the tube hydroforming and the two variations as mentioned above. In contrast to the tube hydroforming, in which expansion is the main method for tube to be formed into the desired shape, bending does play the essential function for tube to be formed into the required shape during the LPTH. In addition, the role of the internal pressure was translated into the function of supporting. All of these brought great convenience to overcome the difficulties as mentioned above. As a result, LPSH and LPTH have obtained a more wide application and development.

Huang investigated the plastic f1ow pattern of a circular tube crushed into rectangular or triangular cross-section [8]. Li revealed the effects of die closing seam [9]. Similar study performed by Nikhare on the simple square shape geometry during low pressure tube hydroforming and found that only 50% of die closing force was enough to form the component than the high pressure tube hydroforming [10]. Lei explored the formability and the potential fracture location during a circular tube expanded into a triangular cross-section [11]. Yang studied the influences of pulsating pressure on the shape precision, the thickness distribution, and the microstructures [12]. Xie analyzed the effects of supporting pressure on the section shape and the thickness distribution [13]. The difference was compared between the HPTH and the conventional mechanical pressing. Nikhare proposed an analytical model for the prediction of die closing force needed [14]. A subsequent study also performed by Nikhare to predict the minimum pressure required for the LPTH [15].

It should be noted that, for tube hydroforming, the tube blank is formed to the required shape by expansion deformation that means no bending deformation happens during hydroforming process. Consequently, springback does not exist. In contrast, the tube sidewall was bended into the desired shape druing the LPTH. For the existence of the bending moment, springback is unavoidable, which would deteriorate the shape accuracy of the formed member. Especially as the increasing use of the high stress steel, springback becomes more and more serious and noticeable, and needs to investigate deeply. However, the studies that do exist mainly focused on the key process factors and the deformation behavior during the LPTH.

In the present study, theoretical analysis of the springback during the LPTH was developed based on the classical theory of elastic mechanics. Then the primary factors and its effects mechanism were given. Subsequently, simulation and experiment were conducted. The bending moment and the springback were validated with experimental and simulation studies.

Theoretical analysis

Specimen

In view of the fact that straight lines and arcs are the primary shape element of automobile components, a rectangular is selected to be the specimen section shape which consists of straight sidewall and arc sidewall simultaneously. The specimen used in this study is shown in Fig. 1. One side length is 54 mm, equal to the outer diameter of the tube blank. The other is 54 mm-d, where d is the die displacement. Constant internal pressure was used in this study.

Both integrated measurement and local measurement are used to evaluate the springback, as shown in Fig. 2. The integrated springback, marked as Δh, is characterized by the difference in vertical height between the target shape and the shape after springback. The local springback is characterized by the variation in the radius of Point C which is the middle point of the corner.

Analytical model

For LPTH, the friction can be ignored for the internal pressure used is far less than the material stress [5]. In addition, a perfect circular arc was assumed in this study, since a previous

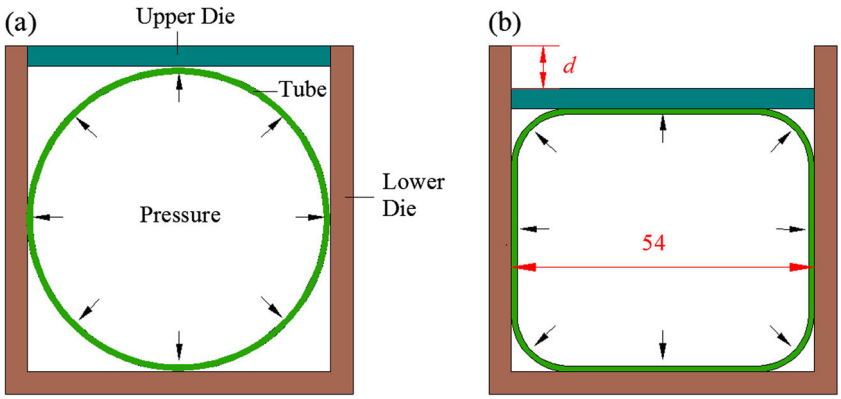

Fig. 1 Schematic of the specimen: **a** before deformation; **b** after deformation

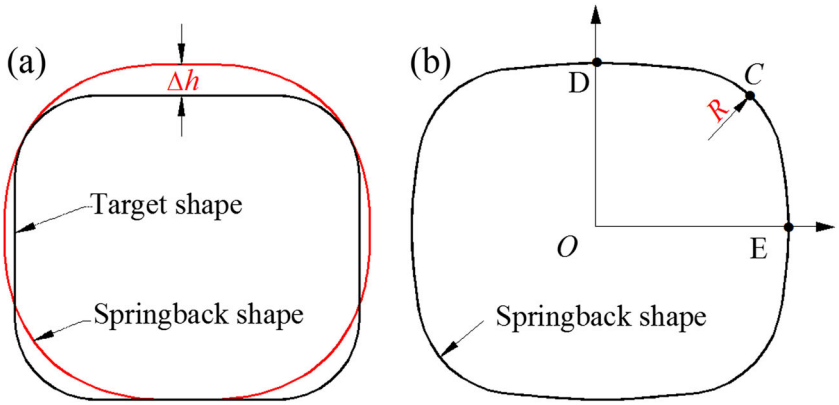

Fig. 2 Measurement of springback: **a** Integrated springback; **b** Local springback

study has shown the arc at the corner stays circular with negligible geometrical error [14]. Applying the advantage of symmetry, only one-quarter of the tube was considered, as shown in Fig. 3a. At the same time, the movement of stress and strain neutral layers was ignored due to the thin thickness of automotive component.

Mechanical analysis

To better understand the force state when the tube crushed among die cavity, the expansion deformation, for which the dies keep closed during tube expanded, was considered and analyzed first. During tube expansion deformation, the straight sidewall AD is acted by both the internal pressure p and the die supporting force p_n. In addition, a point force T also acts on both ends of the straight sidewall AD, which represents the interaction force between the straight line and the circular arc. For the internal pressure p and the die supporting force p_n are the action and the reaction respectively, p must be equal to p_n. Moreover, the distribution both of p and p_n is uniform along the whole straight sidewall.

In contrast, for the LPTH, the corner radius at point C reduces gradually as the upper die moving down, resulting in a reaction force F at point A (Fig. 3c). The arc is straightened at points A and B. Consequently, bending moment introduces at points A, B and C. According to the Ref. [14], the magnitudes of the bending moments at points A, B and C can be assumed the same.

Due to the moment at point A on the straight sidewall AD acts counter clockwise, the material near point A, must has the trend to move away from the die inner surface. As a result, the die supporting force p_n is less than the internal pressure p. However, it needs to note that the affected zone is only among a limited zone. To facilitate the description, mark the affected zone as AJ, which means $p_n<p$ and $p_n=p$ among the zone AJ and zone DJ respectively.

The force states of expansion and LPTH are shown in Fig. 4. In contrast to expansion deformation, the tube is acted

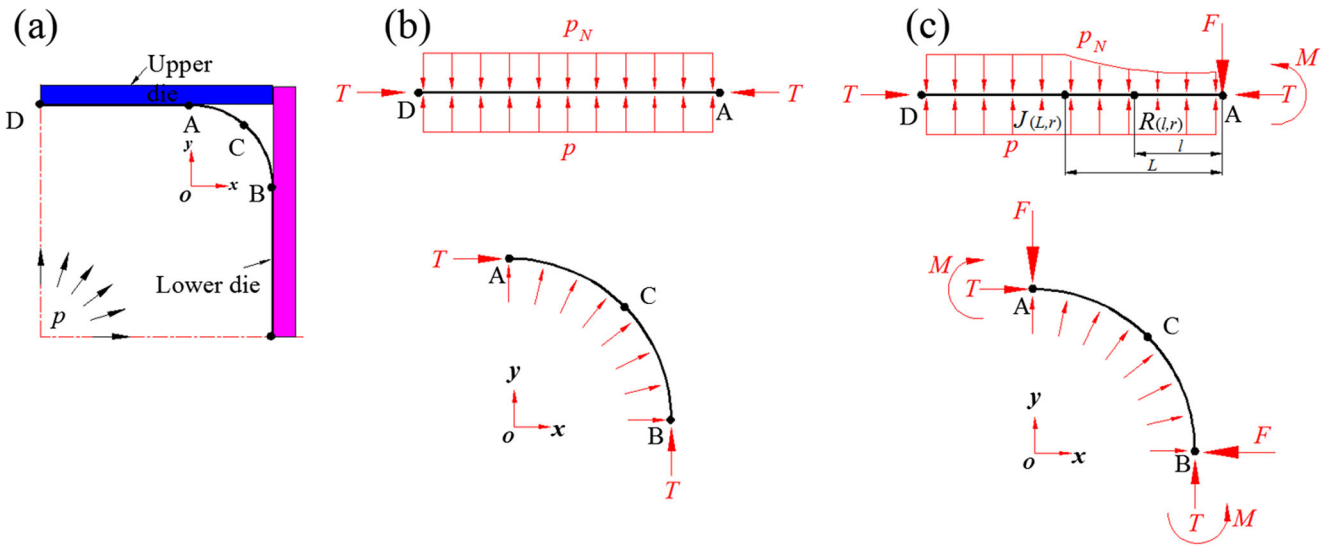

Fig. 3 Force on the quarter of the tube: **a** One-quarter of the tube; **b** Force of expansion deformation; **c** Force of crushing expansion

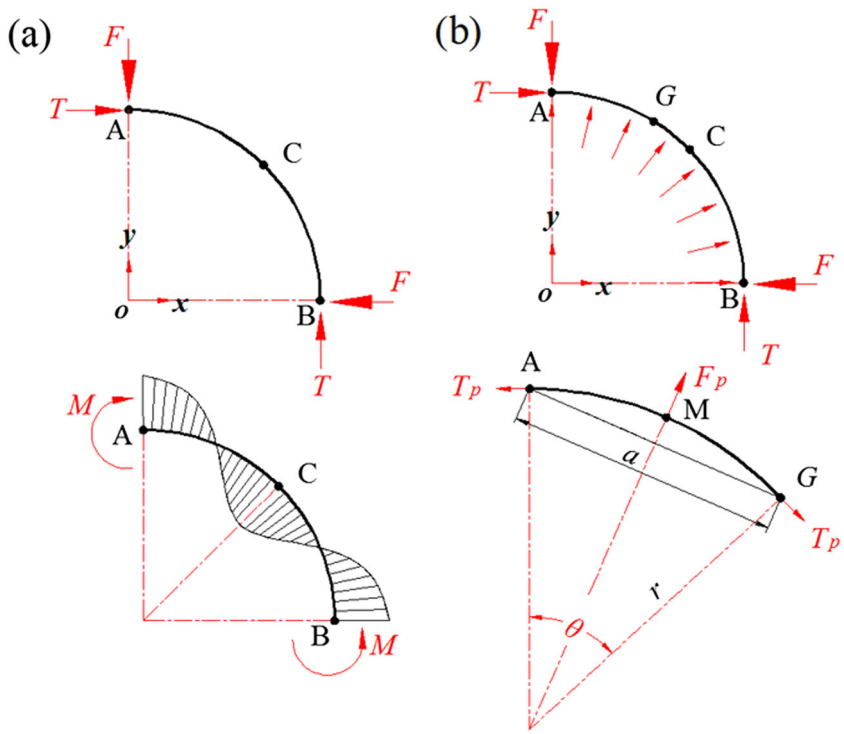

Fig. 4 Forces and moments acting on corner radius: **a** Acting on the unsupported corner radius; **b** Acting on the supported corner radius

by both bending moment and point force at the same time when formed by the moving die.

Bending moment analysis

According to the classic bending theory, springback is directly related with the magnitude of the bending moment (Eq. (17)). Thus, it is the basic problem to explore the distribution of the moment and also its characters.

Bending moment distribution on the straight sidewall

Mark the coordinate of Point J as (L, r), then the bending moment of a random point R(l,r), locates between Points A and D, can be derived as

$$M_R = M_0 - Fl + \int_0^l (p - p_N) x dx \tag{1}$$

Where, M_R is the moment at Point R, M_0 is the moment at Point A.

According to the force equilibrium condition along y direction, the supporting force F can be derived as

$$F = \int_0^L (p - p_N) dx \tag{2}$$

Substitute Eq. (2) in Eq. (1), M_R can be described as

$$M_R = M_0 - \int_0^L (p - p_N) l dx + \int_0^l (p - p_N) x dx \tag{3}$$

If Point A locates between Points A and J, i.e., $l<L$, the relation between M_R and M_0 can be derived as

$$\begin{aligned} M_R &< M_0 - \int_0^L (p - p_N) l dx + \int_0^l (p - p_N) l dx \\ &= M_0 - \int_0^{L-l} (p - p_N) l dx \\ &< M_0 \end{aligned} \tag{4}$$

If Point A locates between Points J and D, i.e., $l>L$, $p_n = p$ at the zone AJ, but $p_n<p$ at zone DJ. Thus, the relation between M_R and M_0 can be derived as

$$\begin{aligned} M_R &= M_0 - \int_0^L (p - p_N) l dx + \int_0^L (p - p_N) x dx + \int_{l-L}^l (p - p) x dx \\ &= M_0 - \int_0^L (p - p_N) l dx + \int_0^L (p - p_N) x dx \\ &< M_0 - \int_0^L (p - p_N) l dx + \int_0^L (p - p_N) l dx \\ &= M_0 \end{aligned} \tag{5}$$

From Eqs. (4) and (5), it can be found that the bending moment of any point on the straight sidewall is always less than that at point A.

Bending moment distribution on the circular arc sidewall

Ref. [14] has developed the bending moment for a circular arc when crushed without internal pressure and points out the bending moments of Points A, B and C can be assumed the same and bigger than that at other points. Figure 4a shows the distribution of the bending moment

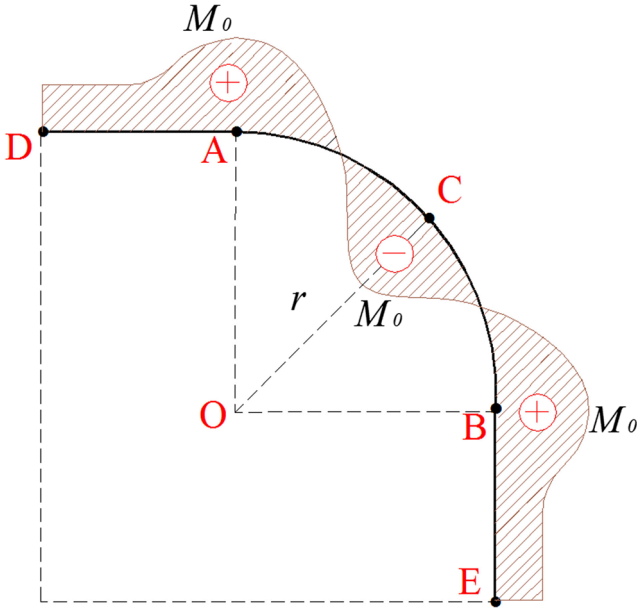

Fig. 5 Bending moment distribution for a tube crushed among a die

for a circular arc when crushed without internal pressure. Different from Ref. [14], the tube in this study was also loaded by an internal pressure. Based on the principle of force addition, it only needs to calculate the moment induced by the internal pressure, and then adds it to the result of Ref. [14].

One half sketch of Fig. 4a is analyzed due to the symmetry of the problem. Point G is a random point locates between Points A and C.

The effects of internal pressure on the circle arc AG consist of two components: one is the pressure directly acting on the arc AG and the other is the tensile force T_p which is the interaction force between the arc AG and the others. In fact, the pressure acting on the arc AG can be equivalent to a point force(F_p) which acts on the middle point M and along the radial direction, as shown in Fig. 4.

According to the equilibrium condition, F_p and T_p, can be derived as:

$$F_P = 2\mathrm{Prsin}\left(\frac{\theta}{2}\right) \tag{6}$$

$$T_P = \mathrm{Pr} \tag{7}$$

M_G can be described as

$$M_G = T_P a\sin(\theta/2) - F_P(a/2) \tag{8}$$

Where, M_G is the bending movement of Point M. Combining Eqs.(6), (7) and (8), we obtain

$$M_G = 0 \tag{9}$$

From Eq. (9), it can be seen there is no bending moment has been introduced when a circular arc acts by the internal pressure. In other words, bending moment distribution for a circular arc acted by the internal pressure is the same with that of no internal pressure acted as shown in Fig. 4a.

In summary, according to the above analysis, the obvious difference between the expansion and LPTH deformations is that bending moment has been introduced. In addition, the bending moments of Points A, B and C are the same and bigger than any other points. Consequently, the distribution of the bending moment for a tube crushed among a die can be drawn as Fig. 5.

Spingback analysis

Due to the springback directly dependent on the magnitude of the bending moment and the fact that Point C has the biggest bending moment, the analysis was mainly focus on Point C in the following study.

According to the above analysis, the bending moments of any points are all related to the bending moment M_0, which brings great convenience to illustrate the moment distribution. In fact, M_0 is a variable related to the internal pressure directly.

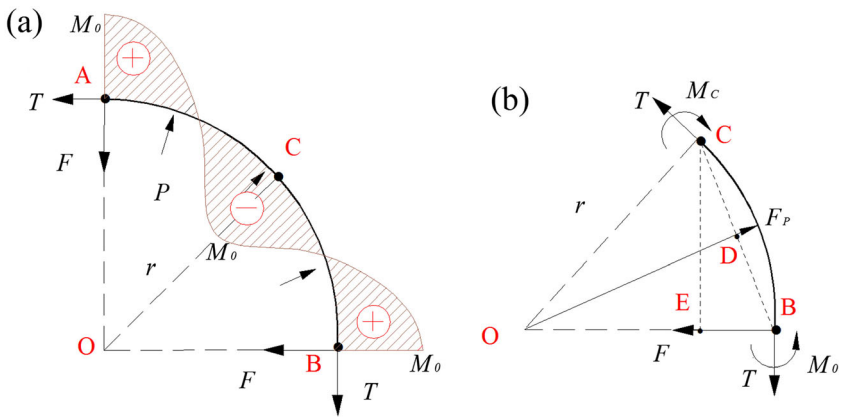

Fig. 6 Forces and moments acting on supportedcorner radius: **a** Schematic of corner; **b** moment at Point C

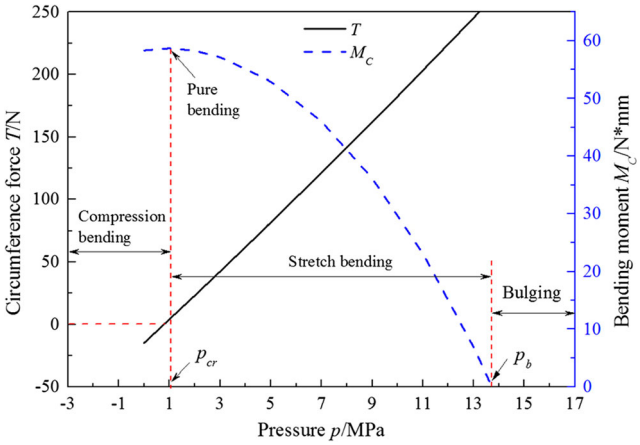

Fig. 7 Effect of internal pressure on tensile force and bending moment

The force analysis was shown in Fig. 6.

Due to the bending moment equilibrium condition, the moment of Point C can be described as

$$M_C = M_0 + F_{pC}\cdot\left(\sqrt{2-\sqrt{2}}\right)/2\cdot r + T\cdot\left(2-\sqrt{2}\right)/2\cdot r - F\cdot\sqrt{2}/2\cdot r \tag{10}$$

$$F = pr - T \tag{11}$$

According to Ref. [],

$$M_C = -M_0 \tag{12}$$

Submitting Eqs. (11), (12) in Eq. (10), the tensile force T can be described as

$$T = pr - \frac{2M_0}{(\sqrt{2}-1)r} \tag{13}$$

In addition, the tensile force T and the bending moment M_0 also have a coupling effect. According to the classic bending theory, the relation can be described as

$$\frac{2M_0}{3M_e} + \frac{T^2}{T^e} = 1 \tag{14}$$

Where, M_e and T_e are the fully elastic bending moment and fully elastic tensile force, which are only related to the material property.

Combining Eqs. (13) and (14), the effect of internal pressure on T and M_0 can be derived

$$T = \frac{(\sqrt{2}-1)T_e{}^2 r}{6M_e}\left(1-\sqrt{1-\frac{12M_e}{(\sqrt{2}-1)T_e{}^2 r}\left[Pr-\frac{3M_e}{(\sqrt{2}-1)r}\right]}\right) \tag{15}$$

$$M_0 = \frac{(\sqrt{2}-1)Pr^2}{2} - \frac{(\sqrt{2}-1)^2 T_e{}^2 r^2}{12M_e}\left(1-\sqrt{1-\frac{12M_e}{(\sqrt{2}-1)T_e{}^2 r}\left[Pr-\frac{3M_e}{(\sqrt{2}-1)r}\right]}\right) \tag{16}$$

Then, the curvature variation before and after springback can be given as

$$\Delta H = \frac{1}{r} - \frac{1}{R} = \frac{M_C}{EI} \tag{17}$$

Where, ΔH is the curvature variation, r is the radius before springback, R is the radius after springback, E is the elastic modulus, I is the inertial moment.

Combining Eqs. (12), (16) and (17), ΔH can be described as

$$\Delta H = \frac{6(\sqrt{2}-1)Pr^2}{Et^3} - \frac{(\sqrt{2}-1)^2 T_e{}^2 r^2}{M_e E t^3}\left(1-\sqrt{1-\frac{12M_e}{(\sqrt{2}-1)T_e{}^2 r}\left[Pr-\frac{3M_e}{(\sqrt{2}-1)r}\right]}\right) \tag{18}$$

Substitute Eq. (18) in Eq. (17), the radius after springback can be given as

$$R = \frac{r}{1-r\Delta H} \tag{19}$$

Form Eqs. (15) and (16) it can be seen that the tensile force T and the bending moment M_0 have a direct relation to the internal pressure. In other words, the internal pressure plays a

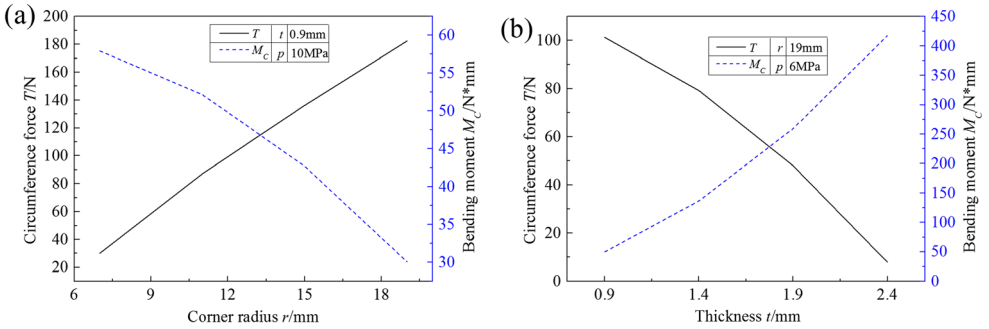

Fig. 8 Effects of corner radius and thickness: (a) Effects of corner radius; (b) Effects of thickness

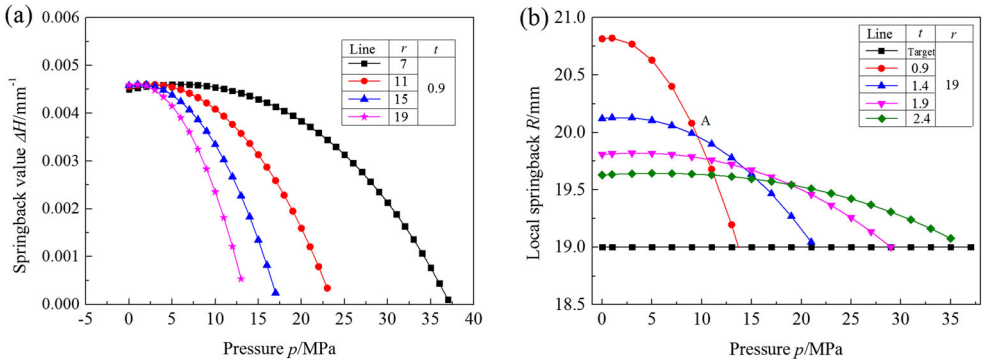

Fig. 9 Effect of internal pressure on springback: (a) Integrated springback; (b) Local springback

useful function to control the loading condition during the LPTH. Consequently, this would make the internal pressure has the function to control the springback due to the relation between bending moment and springback. Form Eq. (18), it also can be seen the radius and the tube thickness also are the key factors for the springback.

Parametric study

Effect of internal pressure on tensile force and bending moment

According to Eqs. (15) and (16), the effects of internal pressure on the tensile force and the bending moment are shown in Fig. 7. One distinct character is that there is a pressure, which lets the tensile force to zero, but the bending moment to reach to the maximum. To facilitate the description, name this pressure as the critical pressure, marked as P_{cr}. It can be seen from Fig. 7, when $p<P_{cr}$, the tensile force is negative which means the tube material is acted by compression force and bending moment, i.e., compression bending deformation happens. On the contrary, when $p>P_{cr}$, the tube material is formed by tensile force and bending moment, i.e., stretch bending deformation happens. When $p = P_{cr}$, pure bending deformation happens. It also can be seen the bending moment decreases to zero at a certain pressure, name this pressure as P_b. In fact, P_b is the pressure needed for bulging deformation and can simply describe as $\sigma_s t/r$ [20], where σ_s is the yield stress, t is the tube thickness and r is the corner radius. In other words, when the internal pressure is higher than P_b, bulging deformation happens. All of these demonstrate that internal pressure has the function to control the loading condition during tube crushing forming.

Figure 8 shows the effects of corner radius and thickness on the bending moment. It can be seen clearly that bigger corner radius is helpful to improve the tensile stress and decrease the bending moment for a certain value internal pressure. However, the tensile force T decreases and the bending moment M_C increases as the thickness increasing.

Effect of internal pressure on springback

The effect of internal pressure on springback is shown in Fig. 9. It can be seen as the internal pressure increases, the spingback increases slightly at first, and then decreases. The maximum springback happens at the critical internal pressure. The reason is pure bending deformation happens at p_{cr}. As a result, the springback must reach the maximum according to

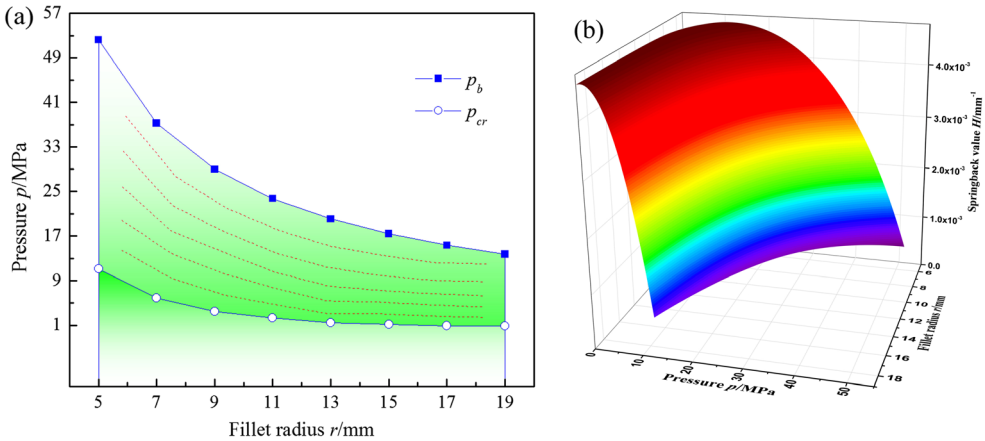

Fig. 10 Critical pressure: **a** Effect of fillet radius **b** 3D graph

Table 1 Mechanical parameters of DP600

Material	Elastic modulus $_E$	Poisson ratio μ	Yield stress σ_s	Tensile stress σ_b
DP600	210GPa	0.3	290 MPa	796 MPa

Eq. (17). From Fig. 9 it also can be seen that there is the same distribution trend of the springback for different corner radius and thicknesses. It needs to note that the internal pressure has a more effective function on suppressing springback when $p>P_{cr}$, and the springback can be eliminated completely when the internal pressure reached P_r.

The critical pressure

From the above analysis, it can be seen that the critical pressure is a key factor for springback which induces the maximum springback and should try to avoid during the LPTH. According to the Eq. (13), the critical pressure P_{cr} can be derived by setting $T=0$. Fig. 10 shows the critical pressure for DP60. It can be seen that bigger corner radius is helpful to decrease the critical pressure. It also can be found the magnitude of the springback reaches the maximum at the critical pressure for any radius and decreases as the pressure moving far away from the critical pressure.

Research procedure

Material and experiment setup

The material used in this study is DP600 tube with the outer diameter of 54 mm. The material properties obtained through tensile test are shown in Table 1 and Fig. 11.

The experimental setup is shown in Fig. 12. One end of the tube was connected to a pressure relief valve which maintained a constant pressure during the forming process, while the other was connected to a hydraulic pressure source. The pressurized tube was placed between the lower and the upper dies and formed to the desired shape by controlling the die displacement d.

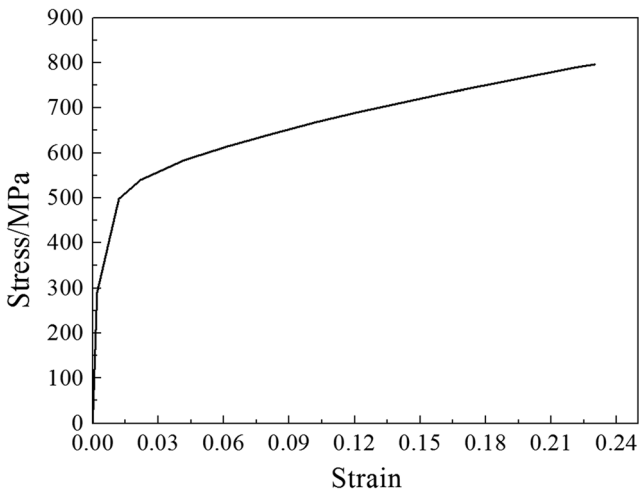

Fig. 11 Material properties of DP600

The height of the specimen after springback was measured by a height ruler. Then the integrated springback Δh can be achieved by comparing the difference in vertical height between the target shape and the shape after springback. The local springback r is characterized by the variation in the radius of Point C which is the middle point of the corner. The cross section of the specimen was input to the AutoCAD, and then the radius of Point C can be measured.

Finite element model

ABAQUS/Explicit version 6.13–1 was used to simulate the plastic deformation to investigate the effect of internal pressure on the bending moment distribution and so on. The ABAQUS/Standard was used to simulate the springback.. According to the research of Ref. [16], the axial strain is close to zero when the tube is formed into a rectangular cross-section, which means the strain state of the tube can be regard as plane strain state. As well known, in this case, the study can be focused on only a segment of the forming zone, which is reasonable and more convenient for the analysis. Consequently, only the upsetting zone was modeled in this study. Considering the plane strain state, two symmetry constraints were applied on both tube ends as shown in Fig. 13. The dies were modeled as analytical rigid body. While, the tube was discretized by elastic-plastic quadrilateral shell elements with the element type of S4R,the element size was about 1 mm and 3 mm for the tube blank and the die respectively, and 5 integral points in the thickness direction. An isotropic plasticity model was applied in the simulation. The material properties used in the numerical simulation was obtained through uniaxial tensile test as shown in Fig. 11. Considering the internal pressure needed in LPTH is far less than the material stress, the forming process was assumed to be frictionless, which has been prove to be acceptable and convenient according to the Refs. [17–19].

Verification and discussion

Figure 14 shows the formed specimens under the pressure of 10 MPa. Springback can be found clearly on the straight sidewall from Fig. 15b. What needs to explain is that springback is

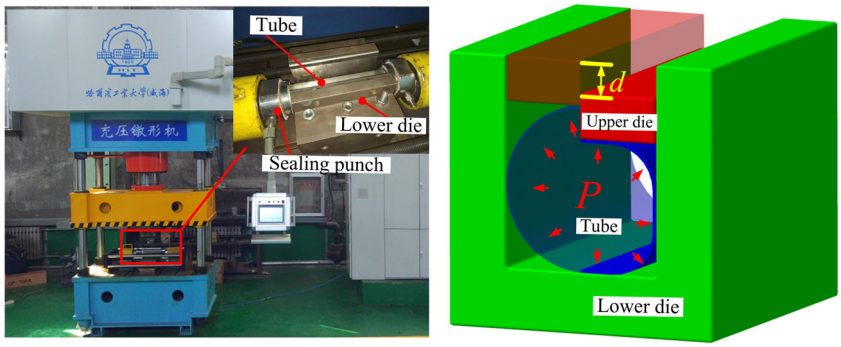

Fig. 12 Experimental setup

more obvious on the corner zone, but is difficult to be observed directly.

From the above theoretical analysis, it illustrates that the internal pressure, the radius and the tube thickness are the three key factors for the springback. Follows, the effects of the three factors according to the experimental and simulation results will be discussed in detail.

Effect of internal pressure on bending moment

The effect of the internal pressure on the bending moment is shown in Fig. 15. Different from the other simulation in this study, the material was assigned as rigid plastic in this section which is necessary to get an independent and absolute effect of the internal pressure and avoid introducing the effects of deformation strengthening.

It can be seen the magnitudes of bending moment at Points A, B and C (shown in Fig. 3a) are about the same, which proves that it is reasonable for the hypothesis of the bending moment in Section "Material and experiment setup". From Fig. 15, it also can be seen the bending moment reaches the maximum at $p = 1$ MPa, after then decrease as the internal pressure improves, which are agreed well with the theoretical results.

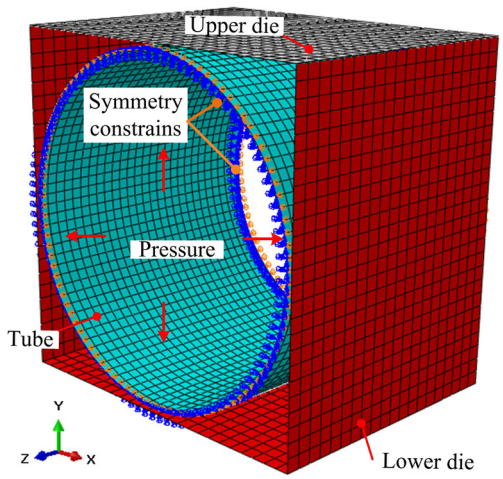

Fig. 13 Finite element model

Effect of internal pressure on springback

In Fig. 16a, the springback is illustrated by the variation of the section shape. It can be seen Δh reaches 2.1 mm, which is already bigger than the tube initial thickness. For such value, the subsequent welding assembly would be seriously affected. Consequently, attentions need to pay on the problem of springback.

Figure 16b shows the comparison between the theoretical, simulation and experimental results. It can be seen both the simulation and experimental results all illustrate that obvious springback happens during the LPTH. Springback reaches the maximum at the critical pressure and decreases as the internal pressure improving. There is good agreement between the theoretical and experimental results. Form the experimental result, it can be seen Δh reaches 2.14 mm when the internal pressure is 1 MPa, and finally disappeares when the internal pressure increased to 14.5 MPa for DP600 tube.

Relation between corner radius and springback

Form Fig. 16, it also can be seen the effect of corner radius on the springback, where the tube thickness is 0.9 mm and the internal pressure is 10 MPa. The springback decreases gradually as the increase of the corner radius. For example, although the same internal pressure has been applied, the springback Δh is 1.96 mm when the corner radius is 7 mm, but decreases to 1.04 mm when the corner radius is 19 mm, which has been decreased by 46.9%. Such effect characters are different from the regularity of springback in conventional sheet forming process, in which the springback increases as the radius increases.

The main reason can be found according to the theoretical analysis result. From Fig. 8a, it can be found that, for a certain internal pressure, bigger corner radius induces a much bigger tensile force but less bending moment. According to Eq.(17), the less bending moment must results the less springback. These also illustrate the useful function of the internal pressure during the LPTH.

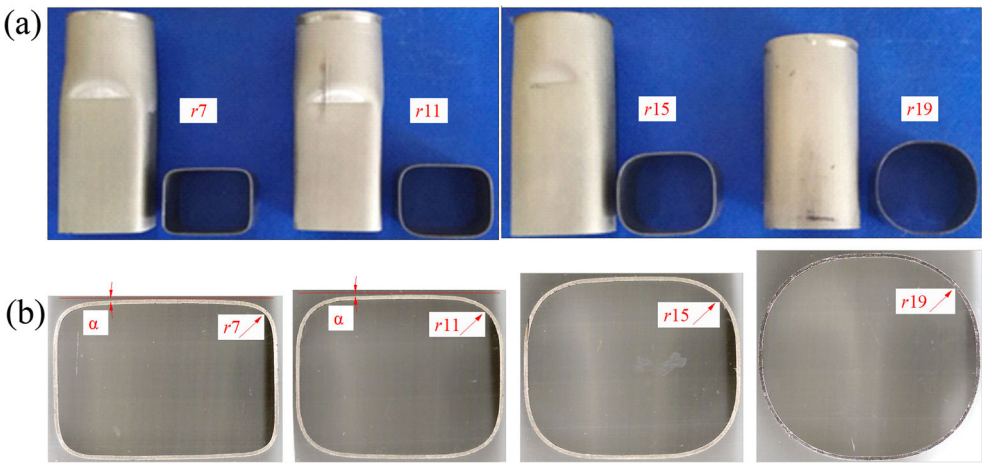

Fig. 14 Specimen with different corner radius: **a** Photo of specimens **b** Cross sections

Relation between thickness and springback

Form Fig. 17, it can be seen that the influence of the wall thickness on springback is much more complex. When the internal pressure is lower, the springback increases as the thickness increases. However, the springback decreases as the thickness increases when the internal pressure reaching a higher degree. For example, the springback of the specimens

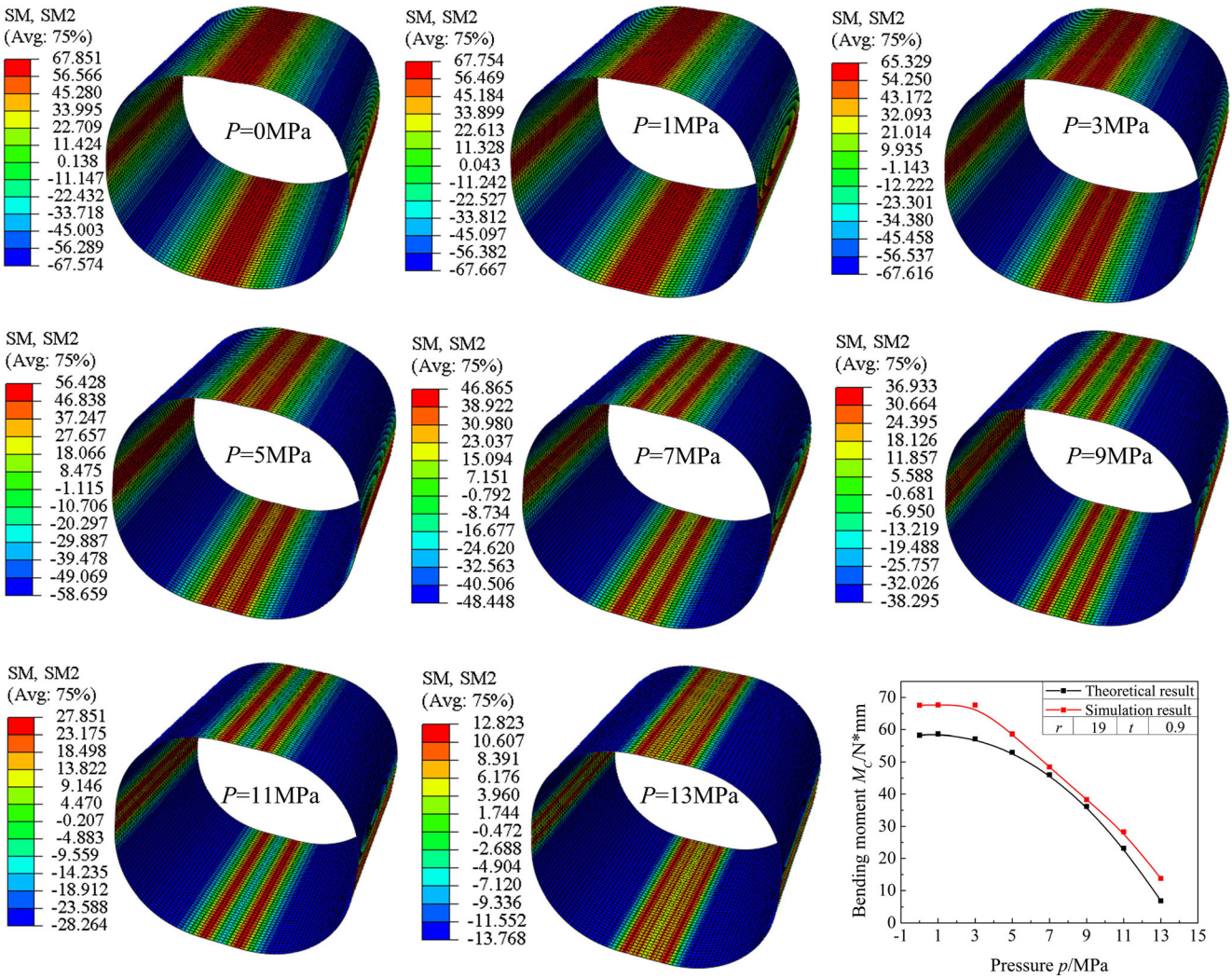

Fig. 15 Simulation results of bending moments

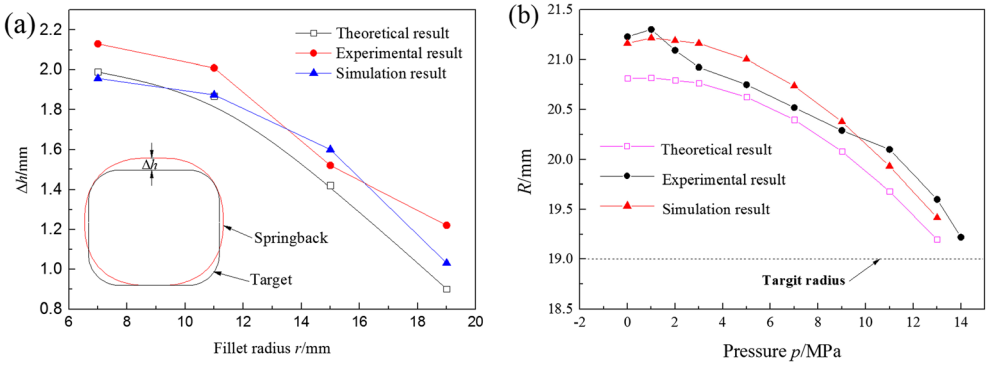

Fig. 16 Effects of internal pressure on springback: **a** Integrated springback; **b** Local springback

with thickness of 0.9 mm is bigger than that of 1.4 mm when the pressure is less than 7.5 MPa, but less than that of 1.4 mm after the pressure bigger than 7.5 MPa. The reason is internal pressure has a more obvious effect on thinner component as shown in Fig. 9b. Consequently, the decline tendency of the springback is more pronounced for the thinner tube as the internal pressure improving as shown in Fig. 17. As a result, the springback of the thinner tube can be decreased to a lower degree after the internal pressure reaching a certain degree.

Critical pressure

As discussed above, P_{cr} is a deteriorated value for the internal pressure and need to avoid during tube crushing forming, especially for the thinner tube. Figure 18 presents the curves of critical pressure *vs* corner radius according to the theoretical and experimental results. The minimum and the maximum pressure for low pressure hydroforming have been given in Refs. [15] and [20]. Combining the result of the critical pressure, the diagram of the loading path can be built. It can be found that the tendency of the critical pressure obtained from the simulation is the same as obtained by the theoretical prediction. The critical pressure decreases as the corner radius increases. Low critical pressure is conducive to a less springback. Thus, it is more reasonable and feasible to use a relative lower pressure in the practical process. It also can be concluded that it is more reasonable and should try to use bigger corner radius for component in the design phase. Otherwise, improving the internal pressure is the only method to decrease the springback if the shape and the material of the component are identified.

Conclusions

1. During the LPTH, there is a critical pressure and should try to avoid for the bending moment reaches to the maximum at such pressure. When the internal pressure is less than the critical pressure, compression bending deformation happens. On the contrary, stretch bending deformation happens. As a result, the maximum springback happens at the internal pressure equal to the critical pressure.
2. During the LPTH, the tube is acted by both a point force and a bending moment simultaneously. The internal

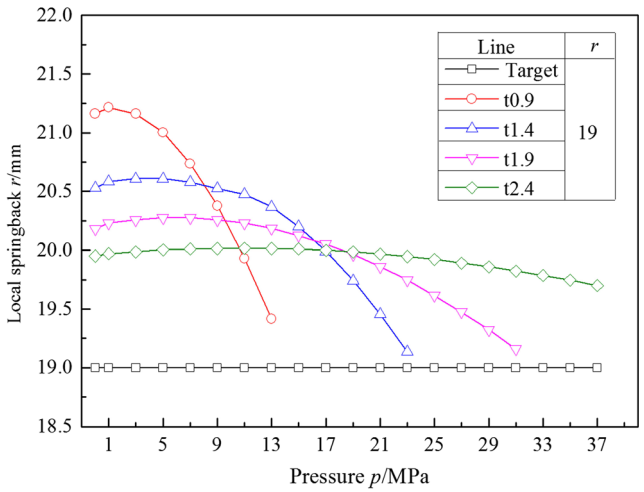

Fig. 17 Effect of thickness on springback according to simulation results

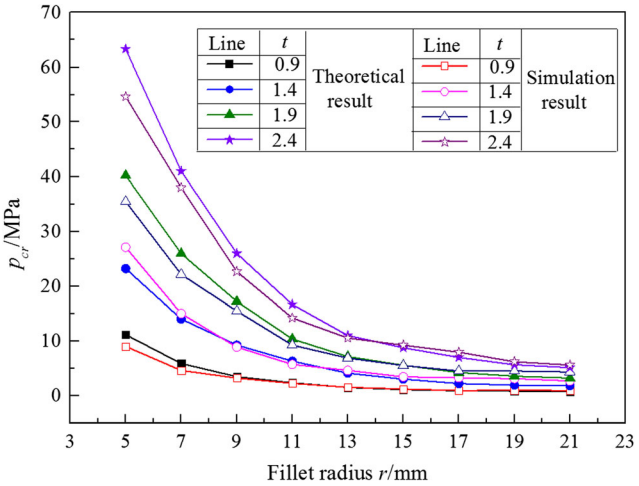

Fig. 18 Critical pressure vs. fillet radius for various *t*

pressure plays a decisive function for the force state. As the increasing of internal pressure, the point force translates gradually from compression force to tensile force and the corresponding bending moment increases at first and then decreases. These make the internal pressure has the function to control the force state and then the springback. In contrast, it is more effective for springback suppression when pressure is bigger than the critical pressure.

3. Corner radius is another key factor for springback. For a certain internal pressure, springback decreases as the corner radius increases. Moreover, the effect of internal pressure is more obvious and effective for the relative bigger corner component.
4. Different from the springback of traditional sheet forming, in which the springback decreases as the increasing of thickness, the relation between springback and thickness is complex during LPTH and LSHT. The suppression of internal pressure on springback is more effective for the thinner tube, which explained why the springback of thinner thickness was bigger than that of thinker thickness under lower pressure, but opposite under higher pressure. For the component with the identified shape and materials, improving the internal pressure is the only method to decrease the springback.

Acknowledgments This study was financially supported by the National Natural Science Foundation of China (Grant No.51475121 and No. 51775134). The authors would like to take this opportunity to express their sincere appreciation to these funding organizations.

Compliance with Ethical Standards

Conflict of Interest The authors declare that they have no conflict of interest.

References

1. Lang LH, Wang ZR, Kang DC, Yuan SJ, Zhang SH, Danckert J, Nielsen KB (2004) Hydroforming highlights: sheet hydroforming and tube hydroforming. J Mater Process Technol 151(1–3):165–177
2. Dohman F, Hartl C (1996) Hydroforming – A method to manufacture light-weight parts. J Mater Process Technol 60:669–676
3. Tang ZJ, He ZB, Liu G, Yuan SJ, Hu L (2009) Hydroforming of AZ61A tubular component with various cross-section. Trans Nonferrous Metals Soc China 19(s):398–402
4. Morphy G (1998) Pressure-Sequence and High-Pressure Hydro-Forming. Tube and Pipe Journal 2(1):128–135
5. Nikhare C, Weiss M, Hodgson PD (2008) Numerical investigation of high and low pressure tube hydroforming. Numisheet Conference Proceedings, Switzerland, pp 691–696
6. Nikhare C, Weiss M, Hodgson PD (2008) Experimental and numerical investigation of low pressure tube hydroforming on stainless steel. Metal Forming Conference Proceedings, Poland, pp 272–279
7. Hwang YM, Altan T (2003) Finite element analyses of tube hydroforming processes in a rectangular die. Finite Elem Anal Des 39(11):1071–1082
8. Hwang YM, Altan T (2002) FE simulation of crushing of circular tubes into triangular cross-setions. J Mater Process Technol 125-126:833–838
9. Li SH, Xu XH, Zhang WG, Lin ZQ (2009) Study on the crushing and hydroforming processes of tubes in a trapezoid-sectional die. Int J Adv Manuf Technol 43:67–77
10. Nikhare C, Weiss M, Hodgson PD (2009) FEA Comparison of High and Low Pressure Tube Hydroforming of TRIP Steel. Comput Mater Sci 47(1):146–152
11. Lei P, Yang LF, Zhang YX (2011) Investigation on the Formability of Tube in Hydroforming with Radical Crushing under Simple Loading Paths. Adv Mater Res 291-294:595–600
12. Yang LF, Rong HS, He YL (2014) Deformation Behavior of a Thin-Walled Tube in Hydroforming with Radial Crushing Under Pulsating Hydraulic Pressure. J Mater Eng Perform 23(2):429–438
13. Xie WC, Han C, Chu GN, Yuan SJ (2015) Research on hydro-pressing process of closed section tubular parts. Int J Adv Manuf Technol 80:1149–1157
14. Nikhare C, Weiss M, Hodgson PD (2010) Die closing force during low pressure tubehydroforming. J Mater Process Technol 210: 2238–2244
15. Nikhare C, Weiss M, Hodgson PD (2017) Buckling in low pressure tube hydroforming. J Manuf Process 28:1–10
16. Yang C, Ngaile G (2008) Analytical model for planar tube hydroforming: prediction of formed shape, corner fill, wall thinning and forming pressure. Int J Mech Sci 50:1263–1279
17. Hwang YM, Altan T (2002) FE simulation of the crushing of circular tubes in triangular cross-sections. J Mater Process Technol 125–126:833–838
18. Hwang YM, Altan T (2003) Finite element analyses of tube hydroforming processes in a rectangular die. Finite Elem Anal Des 39(11):1071–1082
19. Nikhare C, Weiss M, Hodgson PD (2009) FEA comparison of high and low pressure tube hydroforming of TRIP steel. Comput Mater Sci 47:146–152
20. Liu G, Yuan SJ, Teng BG (2006) Analysis of thinning at the transition corner in tube hydroforming. J Mater Process Technol 177(1–3):688–691